

Cancer stem cells recapitulates the heterogeneity of glioblastomas

Abstract

Glioblastoma (GBM) tumor is the most aggressive and heterogeneous cancer originating from the Central Nervous System (CNS). It is not clear how this tumor heterogeneity comes about. The cancer stem cells (CSCs) theory dictates that GBM tumors may arise from a small pool of cells that determine the cancer progression. In this work, we demonstrate that isolated CSCs from single GBM-derived neurospheres give rise to several clones with different proliferation rates *in vitro*. Moreover, the tumors generated by xenografts of these clones, displayed histological features of GBM with different growth rates, which reflect the proliferation kinetics of the injected clones. These results indicate that exist differences in the tumorigenic capacity of CSCs derived from the same single neurosphere, suggesting a possible combination of the cancer stem cells hypothesis and clonal evolution model in generating GBM heterogeneity. We than investigated these differences as possibly related to the distinct expression of transcription factors NRSF/REST and Olig2, the equilibrium of which seems to maintain the more aggressive clone in the more tumorigenic status. Our results indicate a possible predictive role of REST since it is up regulated in more proliferative, invasive and less differentiated cells.

Keywords: cancer stem cells, glioblastoma, heterogeneity, clones, rest, olig2

Volume 1 Issue 1 - 2015

Federica Colleoni,¹ Marzia Belicchi,¹ Paola Razini,¹ Mirella Meregalli,¹ Rossella Galli,² Stefania Mazzoleni,² Silvia Brunelli,² Marina Di Segni,³ Domenico Coviello,⁴ Marco Baccarin,³ Bianca Pollo,⁵ Nereo Bresolin,¹ Lorenzo Bello,⁶ Luciano Conti,⁷ Yvan Torrente¹

¹Stem Cell Laboratory, Department of Pathophysiology and Transplantation, Università degli Studi di Milano, Italy

²Stem Cell Research Institute (SCRI) DIBIT-H. S. Raffaele via Olgettina 60, Italy

³Laboratory of Medical Genetics, Fondazione IRCCS Ca' Granda Ospedale Maggiore Policlinico, via F. Sforza 35, 20122 Milan, Italy

⁴Laboratory of Human Genetics and Department of Experimental Medicine, University of Genoa, Genoa, Italy

⁵Divisione di Neurologia-Neuropatologia V Istituto Neurologico C. Besta, via Celoria 11, 20133 Milan, Italy.

⁶Department of Medical Biotechnology and Translational Medicine, Università degli Studi di Milano, Milan, and Humanitas Research Hospital, Rozzano, MI, Italy

⁷Department of Pharmacological and Biomolecular Sciences, Università degli Studi di Milano, via Balzaretti 9, 20133 Milan, Italy

Correspondence: Dr. Torrente Yvan, Department of Pathophysiology and Transplantation, Università degli Studi di Milano, Fondazione IRCCS Ca' Granda Ospedale Maggiore Policlinico, Centro Dino Ferrari, via F. Sforza 35, 20122 Milan, Italy, Tel +39 02 55033874, Fax +39 02 55034723, Email yvan.torrente@unimi.it

Received: August 04, 2015 | **Published:** September 18, 2015

Abbreviations: GBM, glioblastoma; CSCs, cancer stem cells; CNS, central nervous system; CAM, chorioallantoic membrane

Introduction

One characteristic associating all tumor types is the striking variability among the cancer cells within the single tumor.¹ These cancer cells differ in features (size, morphology, antigen expression, and membrane composition) as well as behaviors (proliferation rate, cell-cell interaction, metastatic predisposition and sensitivity to chemotherapy).² Tumor heterogeneity complicates cancer research and treatment since one tumor samples may not be representative of the whole and because its origins are unclear.^{3,4}

Glioblastoma (GBM), as other tumors, exhibits this sort of cell hierarchy, so that not all the neoplastic cells possess the same tumorigenic potential.⁵ From brain tumor tissues can be obtained neurospheres containing a stem-like population that evidences genetic rearrangements, aberrant proliferation and differentiation properties.^{6,7} The number of neurospheres isolated *in vitro* seems to be directly correlated with growth rate and invasive pattern in xenograft tumor.⁸ In addition, different tumors within the same histological group often

contain cells subpopulations with different gene expression profiles that predispose the patients to clinically different outcomes.^{9,10} These findings suggests that tumor environment is not a collection of a homogenous population of cells, but rather is composed of a varied fractions of tumor initiating cells, defined as cancer stem cells (CSCs) which may differ in terms of tumorigenic potential. These cells share the self-renewal and multipotency characteristics of neural stem cells (NSCs) and recapitulate the original tumor upon transplantation in mice.¹¹⁻¹³ Moreover, the majority of human GBMs exhibit resistance to both radio and chemotherapy and they often recur, despite complete surgical resection of the tumor. This recurrence may be attributable to CSCs, which remain after resection, persist after therapies, migrate throughout the brain parenchyma and retain the ability to form tumors in adjacent tissues. The GBM-derived cancer stem cells has also been demonstrated to be resistant to many form of chemotherapeutic agents,¹⁴ and show an increased DNA repair mechanism even after high dose radiotherapy in contrast to the other tumor stromal cells which remain sensitive to radiation.¹⁵ All these evidences suggest that the biological and clinical heterogeneity of GBM can be explained by the cancer stem cells hypothesis.

Several are the factors, especially transcription factors, which seem to be involved in cancer stem cell tumorigenesis. Between them, RE-1 Silencing Transcription Factor (REST) and Oligodendrocyte Lineage Transcription Factor 2 (Olig2) could play a novel possible role. REST (repressor element 1-silencing transcription factor), also known as NRSF (neuron-restricted silencing factor), is a transcriptional repressor that acts as a negative regulator of genes devoted to many aspects of neuronal function.¹⁶⁻¹⁸ This transcription factor is found to be co-express in abnormally high levels of Myc in many human medulloblastomas and the NSCs overexpressing activated Myc and REST/NRSF proteins are blocked in neuronal differentiation and give rise to cerebellar tumors morphologically similar to human medulloblastomas.¹⁹ Recently was demonstrated that REST promotes oncogenic properties of glioblastoma stem cells too, with respect to self-renewal, cellular viability, and invasion and affects survival in mice bearing CSCs-xenograft tumors.^{20,21} The basic helix-loop-helix transcription factor Olig2 is universally expressed in adult human gliomas and, as a major factor in the development of oligodendrocytes, is expressed at the highest levels in low-grade oligodendroglial tumors. In addition, its expression is linked to the formation of high-grade astrocytomas in a genetically modified murine model.²² High level of Olig2 expression was also observed in anaplastic oligodendrogliomas versus GBMs, which are more heterogeneous. Olig2 protein expression is present but inconsistent and generally lower in most other brain tumors and is absent in non-neuroectodermal tumors. The heterogeneity of expression of Olig2 in astrocytomas precludes immunohistochemical classification of individual gliomas by this marker alone.²³

In this work, we analyzed neurospheres derived from several human glioma samples. *In vivo* analysis allowed us to confirm intra-tumor heterogeneity demonstrating that the injection into nude mice of GBM-derived neurospheres obtained from the same biopsy leads to significant differences in tumor growth. After have been verified a high variability in the tumor sphere-forming ability, we manage to obtain single cell clones only from one of all this biopsies, focusing our attention on these peculiar cells. Furthermore, we observed a different expression of the transcription factors REST and Olig2 among these clones, suggesting a possible relationship between transcription factors, stemness and tumorigenicity of the single clones. Moreover, these proliferating differences were mirrored in xenografts, which displayed histological features of the original GBM with different tumor growth rates reflecting their proliferation kinetics.

Material and methods

Sample classification

All of the tumor clinical biopsies were collected from surgery resections of patients after informed consent, according to the guidelines of the Committee on the Use of Human Subjects in Research of the Fondazione IRCCS Ca' Granda Ospedale Maggiore Policlinico (Milan, Italy). The samples were obtained from 78 patients with diagnosis of different grade of astrocytomas: 46 derived from patient suffering of primary glioblastomas; 12 were obtained from glioblastoma recurrences and underwent chemotherapy/radiotherapy before surgery; 12 from astrocytomas grade III WHO/Anaplastic astrocytomas and 8 from astrocytoma II WHO.

Primary tumor sphere culture, propagation and cloning

Cells were isolated from human tumor processed immediately

after surgery. Biopsies were treated as previously described.^{24,25} Primary cells were plated onto an untreated 6-well tissue culture plate in Dulbecco's modified Eagle's medium (DMEM)/F-12 medium (1:1) (Euroclone, Irvine, Scotland) containing of 20ng/ml human recombinant EGF (Sigma-Aldrich, Saint Louis, Mo, USA) and 10ng/ml human recombinant fibroblast growth factor (FGF2, Sigma-Aldrich, Saint Louis, Mo, USA) whose nutrient composition is optimized for neural stem cell growth. In these conditions, cells rapidly grow to form neurospheres. After 4days, cultures were collected, mechanically dissociated and single cells re-plated in the same conditions. Bulk cultures were generated by passaging the cells at higher density (1×10^4 cells/cm²) every 3-4days in the same growth medium. Cell number and viability were determined at every passage with a Burker's camera by trypan blue exclusion. In differentiation experiments the floating spheres were harvested, dissociated, and plated on collagen-coated wells in NeuroCult NS-A Basal medium (Stem Cell Technologies, Vancouver, Canada, Vancouver, Canada, Vancouver, Canada) added with 10% neurocult NS-A differentiation supplements (Gibco-BRL, Grand Island, NY-BRL, Grand Island, NY, Grand Island, NY) and cultured for 3 weeks. To obtain single cell clones, primary tumor spheres of 100-200 cells/sphere were dissociated and single cells plated by limiting dilution in 96-well plates in 0.1ml/well of serum-free neural stem cell medium. Only wells containing single cells were considered. Proliferation curve was obtained measuring viable cell number on days 1, 4, 7, 12, 18, 25 and 32.

Evaluation of tumorigenicity by chicken chorioallantoic membrane experiments

Experimental glioma growth was obtained after grafting 10^6 cells from 021 neurospheres, clones and 0627 (positive control cell line) in 20 μ L of medium on the chorioallantoic membrane as described previously.²⁶ Seven days after cells implantation, membranes were carefully harvested and frozen in liquid nitrogen-cooled isopentane for cryostat sectioning and histological analysis.

Evaluation of tumorigenicity by orthotopic injection in nude mice

For the intracranial glioma model, 6-week-old nude mice (Charles Rivers Italia, Calco, Italy) received a stereotactical injection of the cells into the left forebrain (2mm lateral and 1mm anterior to bregma, at a 3 mm depth from the skull surface). All surgical procedures were performed respecting the Italian guidelines concerning the use of laboratory animals. Surgery was carried out in aseptic conditions with the aid of a microscope. Anesthesia was induced by an intraperitoneal injection of chloral hydrate (LGC Standards, Teddington, West London). We injected 34 nude mice with 10^5 cells of the 021 derived neurospheres and sacrificed by at different time points as indicated in the results section. To compare cells behaviour *in vivo* and to test clones tumorigenic abilities, we implanted the same cell number (10^5) of C2 clone (n=10) and F6 clone (n=10) cells. Animals were sacrificed by cervical dislocation after 80 and 100 days of transplantation. During all the experiments period, animals were carefully monitored for the occurrence of any side effects and immediately sacrificed at the occurrence of any neurologic deficits. All brains were removed and frozen in liquid nitrogen-cooled isopentane. Cryostat sections from frozen tissues embedded in freezing medium were cut into 10 μ m serial sections and processed for Hematoxylin and Eosin (H&E) staining or immunofluorescence analysis.

Immunocytochemical and immunofluorescence analysis

Immunofluorescence on differentiated tumor cells was performed both in multiwell and slides after cytospin. Cells were fixed in 4% paraformaldehyde and stained with antibodies against nestin (1:50; BD, San Jose, CA, USA), β -tubulin III (1:50 Sigma- Aldrich, Saint Louis, Mo, USA), GFAP-Cy3 conjugated (1:300, Sigma-Aldrich, Saint Louis, Mo, USA), A₂B₅ (1:100, Chemicon- Millipore, Darmstadt, Germany), REST (1:50 Bethyl Laboratories, Montgomery, TX, USA), Olig2, Sox-2 and NeuN (1:50, Chemicon- Millipore, Darmstadt, Germany). For tissues immunofluorescence analysis, CAM and brain sections were fixed in acetone/ethanol (1:1) and incubated with antibodies anti-lamin A/C (1:100; Novocastra- Leica Microsystems, Wetzlar, Germany) and anti GFAP-Cy3 conjugated (1:300, Sigma-Aldrich, Saint Louis, Mo, USA Aldrich). Proliferating cells were detected by human Ki67 staining (1:100, DAKO- Agilent Technologies, Santa Clara, CA, USA). The sections and the cells were rinsed in PBS and incubated with corresponding secondary antibodies Alexa Fluor 488 or Alexa Fluor 594-conjugated, (1:200, Molecular Probes - Life Technologies - Thermo scientific, Rockford, IL, USA). Cell nuclei were stained with 4',6-diamidino-2-phenylindole (DAPI, Sigma-Aldrich, Saint Louis, Mo, USA). Stained cells and tissues were examined under a Leica TCS-SP2 confocal microscope by Leica Confocal Software and Leica fluorescent microscope DMIRE2 by QFluoro Software (Leica Microsystems, Wetzlar, Germany). Quantification of positive cells stained with each antibody was calculated as a percentage of total nuclei counted. Immunohistochemical staining were conducted on sections incubated at room temperature for 20min with a solution of methanol containing 0.03% H₂O₂, for 30 min with 2% horse serum and then for 60min with anti-CD31 antibody (BD, San Jose, CA, USA). After rinse with PBS, sections were incubated with biotinylated secondary antibodies (1:100; Vector Laboratories, Burlingame, CA, USA), washed, and incubated with the avidin-biotinylated peroxidase complex (Vectastain ABC Kit, Vector Laboratories, Burlingame, CA, USA). The staining was developed by 3,3'-diaminobenzidine solution. Sections were counterstained with hematoxylin. For all immunostaining, control reactions were done omitting the primary antibody, which was substituted by non-immune serum.

Karyotype analysis

Cytogenetic study was performed on 4 types of tumor derived cells: biopsy 021 (early passage), biopsy 021 (P20), clone C2 (P3) and clone F6 (P3). Metaphases chromosome were harvested at the designed passages during the exponential phase of growth. We added 20 μ L/mL of Colcemid (Gibco-BRL, Grand Island, NY; 10 μ g/mL) directly to the cultures and samples were incubated for 6 hours in 5% CO₂ at 37°C. Tumor spheres were gently aspirated to disaggregate every hour. Cells were incubated in hypotonic solution (0.6% Na₂Citrate -0.13% KCl, 1:1) at room temperature for 10 minutes followed by short sequential washes with Ibraimov solution (distilled H₂O, 5% and 2 times in methanol/acetic acid (3:1). Cells were fixed at controlled temperature (28°C) and humidity (42% rH), by Optichrome (Euroclone, Irvine, Scotland) instrument. Chromosomes was Q-banded and analyzed under a fluorescent microscope (Olympus BX41) at X 100 magnifications. Metaphases were karyotyped according to ISCN (International System for Human Cytogenetic Nomenclature 2009) using an automated imaging system (CytoVision version 4.02; Applied Imaging Corporation).

Quantitative analysis of REST and Olig2 mRNA expression

For quantification of REST/NRSF and GAPDH genes, total RNA (1 μ g) obtained from proliferating clones derived neurospheres were treated with DNase-RNase free (Promega, Madison, WI, USA) in order to avoid amplification of genomic DNA. Dnase-treated RNAs were retrotranscribed by using Super Script First Strand Synthesis System III for RT-PCR (Invitrogen, Thermo scientific, Rockford, IL, USA) with oligo(dT)₁₆ primers. cDNA (1.5 μ L) was subjected to qRT-PCR using PTC200 Chromo4 MJ Research instrument (Bio-Rad Laboratories, Hercules, CA, USA, Hercules, CA, USA). qRT-PCR was performed in 20 μ L volumes using FluoCycle SYBR Master Mix (Euroclone, Irvine, Scotland). All PCR assays were performed in triplicate and the data were pooled. Before using the Δ C_T method for relative quantification, we performed a validation experiment to demonstrating the efficiency of the primers of the target gene. The reaction conditions were as follows: 95°C for 10min; followed by 50 cycles at 95°C for 15s (denaturation) and 60°C for 1min (annealing and elongation). After each experiment Melting Curve from 55.0°C to 95.0°C, ready every 0.5°C was performed. Threshold cycle numbers (C_T) were determined using MJ OpticonMonitor Analysis Software and transformed using the Δ CT (2^{- Δ C_T}) comparative method.²⁷ The data were showed as normalized expression (2^{- Δ ACT}). Gene-specific expression values were normalized to expression values of GAPDH gene (endogenous control) within each sample. The sequences of the primer were:

h-REST/NRSF: FW 5' - ACT TTG TCC TTA
CTC AAG TTC TCA - 3'

REV 5' - GCA TGG CGG GTT ACT TCA TGT T - 3'

h-Olig2: FW 5' -
CGTCGTCCACCAAGAAGGAC - 3'

REV 5' - TGTGCGTACGGCATGACCTC - 3'

GAPDH: FW 5' - AGC TGA ACG GGA
AGC TCA CT - 3'

REV 5' - AGG TCC ACC ACT GAC ACG TTG - 3'

Western blot analysis of REST expression

For Western blot analysis cells were lysed directly in 1X sample buffer (2% SDS) added with commercially available cocktails of protease and phosphatase inhibitors (Complete and PhosSTOP respectively, both from Roche, Mannheim, Germany). Lysates were boiled 5 min and centrifuged at 10000xg for 5min to remove insoluble material. Total protein concentration was determined according to Lowry's method.²⁸ Samples were analyzed on 7.5% polyacrylamide gel, transferred to supported nitrocellulose membranes (Bio-Rad Laboratories, Hercules, CA, USA, Hercules, CA, USA), and the filters were saturated in blocking solution (10mM Tris, pH 7.4, 154mM NaCl, 5% milk, 0.05% Tween-20) for 1 hour at room temperature.

Primary antibodies (anti-REST dilution 1:500 Millipore; anti β -actin dilution 1:100 Sigma-Aldrich, Saint Louis, Mo, USA) were incubated overnight 4°C and then followed by washing, detection with horseradish peroxidase (HRP) conjugated secondary antibodies (DakoCytomation, Carpinteria, CA, USA), and developed by enhanced chemiluminescence (FEMTO) (Thermo scientific, Rockford, IL, USA). Prestained molecular weight markers (Bio-

Rad Laboratories, Hercules, CA, USA) were run on each gel. Bands were visualized by autoradiography using Amersham Hyperfilm (Amersham Biosciences, Piscataway, NJ, USA).

Results and discussion

GBM-derived Cancer Stem Cells isolation and single cells clones analysis revealed inter- and intra- tumor heterogeneity

Tumor biopsies were obtained from 78 patients affected by different staged astrocytomas (grade II to grade IV-GBM). The dissociation of the freshly isolated specimens generally led up to the formation of floating neurospheres within 48 hours. Cytofluorimetric analysis of neurospheres excluded blood contamination. Regardless of tumor subtype (treatment and recurrence), the number of produced neurospheres was very variable, and in some cases the specimens dissociation did not generated any neurosphere. We obtained

neurospheres from 24 biopsies: 22 GBMs samples and 2 grade II astrocytomas (Table 1A). The mean percentage of neurospheres-generating biopsies was assessed around 30%. We then assessed multipotency of clonal tumor derived cells by determining their ability to generate neurons, astrocytes, and oligodendrocytes. Cells needed a mean of 30days to adhere and to start differentiation. By immunofluorescence analysis we observed differentiated GFAP-positive astrocytes (90% of total differentiated cells) and neuron-like cells immunoreactive for β -tubulin III (80% of total differentiated cells) while there was only a minor oligodendrocytes population positive for A₂B₅ antigen (45% of total differentiated cells). As we expected since it has been described in several works, we observed the aberrant differentiation typical of the cancer stem cell, the simultaneous expression of GFAP astrocyte and neuronal β -tubulin III markers in 78% of total differentiated cells. The relative differentiation was similar in all the cellular subtypes considered and such multipotency was maintained unaltered even after extensive culturing (Figure 1 A-I).

Table 1A Summary of biopsies

Biopsy n°	Age (years)	Sex	Istology	Biopsy n°	Age (years)	Sex	Istology
21	73	F	Glioblastoma	108	52	F	Anaplastic astrocitoma III WHO
22	70	F	Glioblastoma	109	59	M	Glioblastoma
26	63	F	Glioblastoma	110	36	F	Anaplastic astrocitoma II WHO
28	42	F	Glioblastoma	111	47	F	Anaplastic astrocitoma III WHO
29	53	M	Glioblastoma	113	63	M	Glioblastoma
30	38	M	Anaplastic astrocitoma III WHO	115	41	M	Anaplastic astrocitoma II WHO
35	60	M	Glioblastoma	116	64	M	Glioblastoma
37	75	F	Glioblastoma	119	37	M	Anaplastic astrocitoma III WHO
38	36	F	Anaplastic astrocitoma III WHO	121	45	M	Glioblastoma
40	76	M	Glioblastoma	124	64	M	Glioblastoma
41	49	M	Astrocitoma II WHO	125	63	M	Glioblastoma
43	72	M	Glioblastoma	128	56	F	Glioblastoma recurrence
44	37	M	Glioblastoma recurrence	129	31	M	Astrocitoma III WHO
47	66	M	Glioblastoma	132	41	M	Glioblastoma
50	25	M	Astrocitoma II WHO	133	44	M	Glioblastoma
51	68	M	Glioblastoma	135	33	F	Astrocitoma III WHO
55	25	M	Astrocitoma II WHO	136	58	F	Glioblastoma recurrence
58	38	M	Glioblastoma	137	50	M	Glioblastoma recurrence
60	70	M	Glioblastoma	138	55	M	Glioblastoma
65	54	M	Glioblastoma recurrence	139	57	F	Glioblastoma
66	45	F	Glioblastoma recurrence	143		F	Glioblastoma
68	62	M	Anaplastic astrocitoma III WHO	146	51	M	Glioblastoma
69	57	M	Glioblastoma recurrence	147	52	F	Glioblastoma
72	68	M	Glioblastoma	149	66	F	Glioblastoma

Table Continued..

Biopsy n°	Age (years)	Sex	Istology	Biopsy n°	Age (years)	Sex	Istology
73	62	F	Glioblastoma	150	68	M	Glioblastoma
74	49	M	Anaplastic astrocitoma	155	38	M	Astrocitoma III WHO
76	54	M	Glioblastoma recurrence	157	49	M	Astrocitoma II WHO
77	34	M	Anaplastic astrocitoma III WHO	159	38	M	Astrocitoma II WHO
78	23	M	Glioblastoma recurrence	165	65	F	Glioblastoma
81	65	F	Glioblastoma	167	24	M	Glioblastoma
82	67	M	Glioblastoma recurrence	168	58	F	Glioblastoma
84		F	Glioblastoma	169	61	F	Glioblastoma
87	52	F	Glioblastoma	171	35	M	Astrocitoma III WHO
94	48	M	Anaplastic astrocitoma II WHO	174	72	F	Glioblastoma
95	60	F	Glioblastoma	175	39	F	Glioblastoma
96	68	M	Glioblastoma	176	32	F	Glioblastoma
100	66	F	Glioblastoma	177	41	M	Glioblastoma
101	60	F	Glioblastoma	180	39	F	Glioblastoma recurrence
104	50	M	Glioblastoma	183	34	F	Glioblastoma recurrence

We attempt to generate single cell clones from the 24 biopsies to obtain more homogeneous cell populations by dissociating primary tumor spheres and plating single cells at serial dilutions down to one cell/well. Clones generation from disaggregated primary cancers spheres provides an index of the cancer clonogenicity and allows determining the number of stem cells within a neurosphere. We obtained a clonal frequency of 33,3 % (60 actively proliferating single cell clones) while the 22,2% died after few passages and the 44,4% remained quiescent. In these experiments, we are able to obtain viable and proliferating clones only from 021 biopsy (as summarized in the Table 1B) and we consequently focused the subsequent experiments on this biopsy.

Table 1B Main chromosomal abnormalities observed*

	46 Primary GBM
	11 Recurrence GBM
78 Biopsies	13 Astrocytoma III
	8 Astrocytoma II
	22 GBM
24 Neurospheres-generating biopsies	0 Astrocytoma III
	2 Astrocytoma II
1 clonogenic biopsy	1 GBM 021

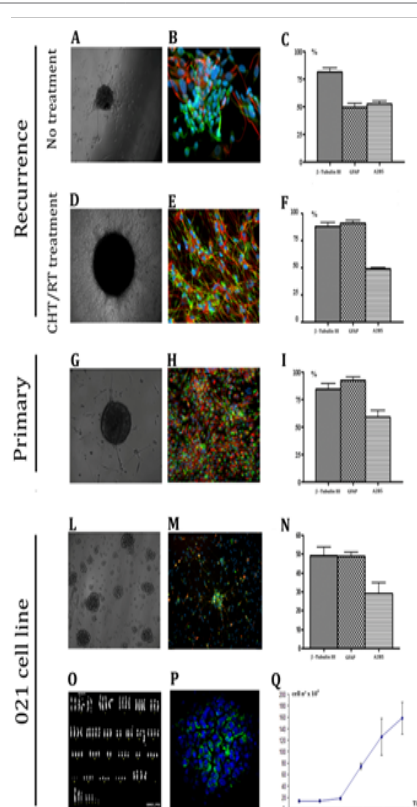


Figure 1 Neurospheres obtained from different staged gliomas retain similar differentiation capacity *in vitro*. Biopsies obtained from different grade of gliomas give rise to neurospheres *in vitro* (A-D-G). Tumor derived neurospheres differentiate in cells co-expressing β -tubulin III (in green) and GFAP (in red) (B,E,H) magnification 20X. The relative percentage of differentiation is shown in C,F,I. Cells derived from the dissociation of 021 tumor specimen grow in neurospheres (L). These cells differentiate in both neural (β -tubulin III in green) and astrocyte (GFAP in red) cells (M) magnification 20X. N, relative percentage of differentiation in the three neural lineages. 021 GBM-derived neurospheres (O) shown a near tetraploid karyotype (P), the majority of cells constituting the 021 neurospheres express nestin (green) and grow with exponential proliferation rate (Q).

021 biopsy derived neurospheres (Figure 1L) express stem cell marker nestin (Figure 1P) and showed an aberrant karyotype with a tetraploid like chromosomes content (Figure 1O) as described in the following section. Growth curve of the neurospheres derived from the 021 GBM biopsy was characterized by a rest phase in the first 3 days, followed by exponential rate of proliferation from the fourth day of culture (Figure 1Q). These neurospheres demonstrated their multipotency and were able, under differentiating conditions, to generate neurons (80% of total differentiated cells), astrocytes (90% of total differentiated cells), and oligodendrocytes (45% of total differentiated cells - Figure 1M, 1N). Interestingly, these clones showed different proliferation rates, in fact, 021 GBM derived neurospheres kinetic settled as a mean value between all the clones, the slower being F6 clone and the faster C2; this last one seems to be the responsible of the main proliferating ability of the 021 GBM-derived

neurospheres (Figure 2A). Clones were tested for their stemness properties firstly by mechanical dissociation and all of them generated secondary tumor spheres exhibiting self-renewal ability and then by nestin and Sox2 immunostainings showing an almost total expression of both cytoplasm and nuclear markers, as shown in Figure 2B. All the clones showed a comparable morphology and properly differentiate in the three neural lineages (Figure 2C-D). Furthermore, as the original 021 GBM-derived neurospheres, they showed the aberrant co-expression of neuronal markers (both β -tubulin and NeuN) and glial markers and the maintenance of a basal stemness marker expression, as demonstrated by immunoreaction with anti-nestin antibody. These observations suggest that isolated clones possess similar cancer stem cell characteristics *in vitro* even though they present differences of proliferation rate that need to be investigated *in vivo*.

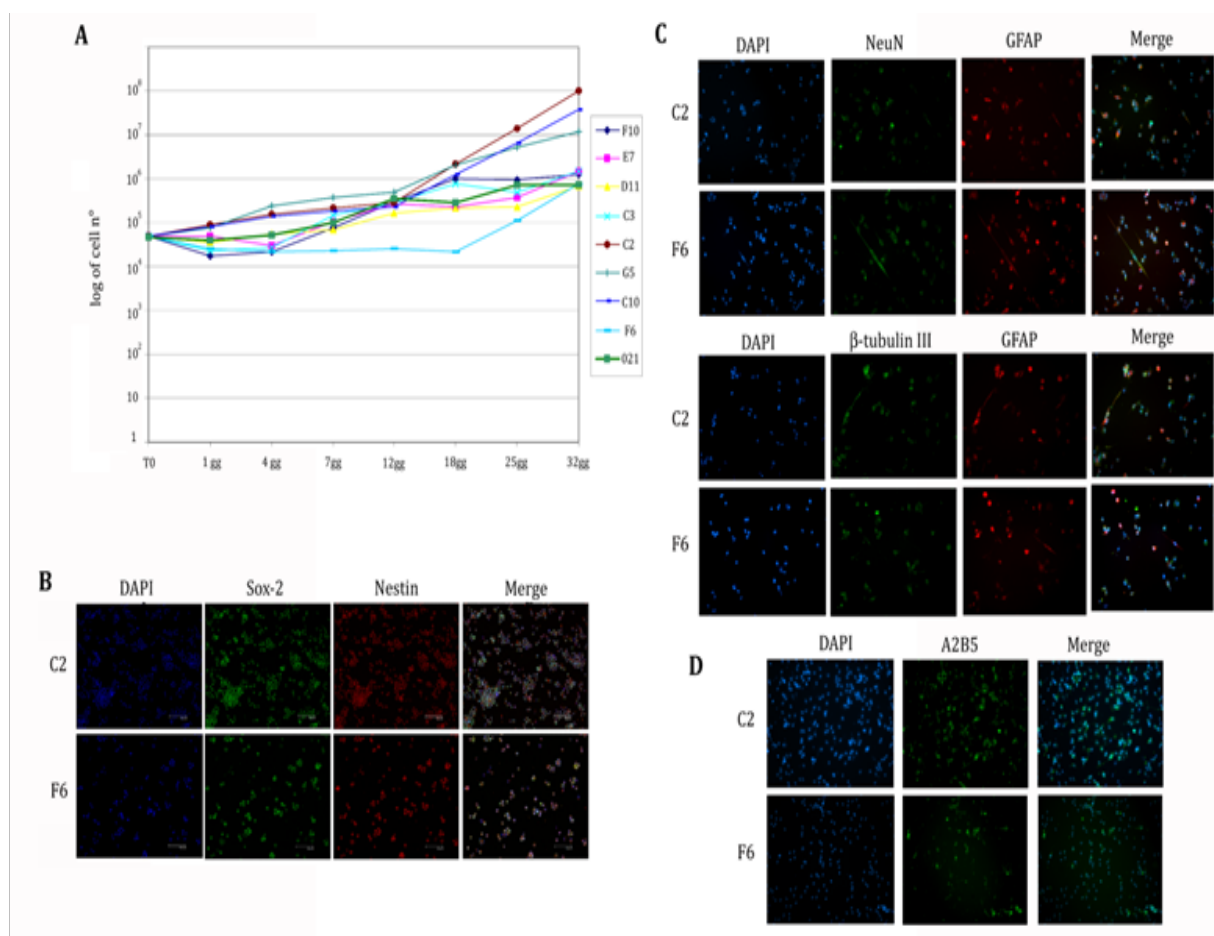


Figure 2 Analysis of clones derived from the 021 GBM-derived neurospheres. In A is shown the proliferation graph show different kinetics of growth. Stemness properties of 021 GBM clones were evidenced by a high expression of the stem cell markers Sox-2 (green) and nestin (red) (B). Multilineage differentiation capacity of the clones were demonstrated by the expression of neuronal (NeuN and β -tubulin–green in C) glial (GFAP–red in C) and oligodendrocyte (A2B5–green in D) markers.

Chicken chorio-allantoic membrane (CAM) model allowed the screening of tumorigenic capacity of clones obtained from the 021 GBM-derived neurospheres

To select the more suitable clones for the *in vivo* implantations and screen their tumorigenic capacity, we built up experiments in the chicken chorioallantoic membrane (CAM). This model was previously described as an ideal environment to study angiogenesis and tumor

growth.^{26,29} In these experiments, we injected 72 total eggs divided as follow: 13 eggs for 021 GBM-derived neurospheres, 12 for 0627 (glioma cell line as control), 12 for D11 clone, 17 for F6 clone, 9 for C2 clone and 9 for E7 clone. The percentage of embryos survival after injection was poor, assessing at 40%. As we harvested the injected membranes, they appeared highly vascularized. The H&E stainings showed the presence of tumor cells clusters and immunofluorescence staining evidenced they express human lamin A/C and GFAP. The

injection of the glioma cell line 0627 (as control - Figure 3A-C), and 021 GBM-derived neurospheres (Figure 3D-F), given rise to similar human cells mass. Interestingly, the clones behaved in different ways: some of them, like the C2 clone, grew in a similar way than the control 0627 and 021 GBM-derived neurospheres, whereas other ones, like F6 clone, gave rise to few dispersed cells within the injected CAM (Figure 3G-I). These data support the differences of the proliferation rates of the clones obtained from the 021 GBM-derived neurospheres.

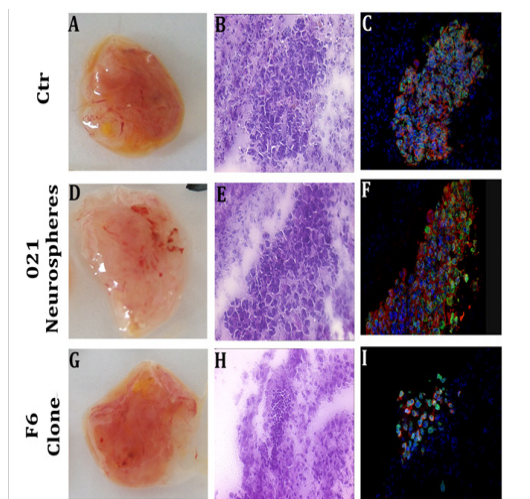


Figure 3 Different cell lines (0627 glioma-derived cell line as control, 021 GBM-derived neurospheres and F6 clone) were tested in chicken chorio allantoic membrane for their tumorigenic ability. In A, D and G CAM as they appear when removed after 5 days of implantation. H&E staining revealed some aggregates of tumor cells in all the samples (B,E,H). Immunofluorescence staining demonstrated the human origin of injected cells (Lamin A/C in green) and their astrocyte commitment (GFAP in red) (C,F,I; magnifications 20X).

Cytogenetic analysis of 021 GBM-derived neurospheres and relative clones shown similar aberrant karyotype

We performed cytogenetic analysis on 021 GBM-derived neurospheres at early and late culture passages to be sure not to introduce some aberration during long periods of *in vitro* culture. Two clones obtained from the 021 GBM-derived neurospheres that showed opposite proliferation rates (F6 and C2) were also tested for specific chromosomal aberration. Four illustrative samples were analyzed (021 GBM-derived neurospheres at early and late culture passages; F6 and C2) and exhibited similar numerical changes of chromosomes and a near-tetraploidy modal number (81-103 chromosomes). Chromosome losses are the most common abnormality mostly involving chromosome 5 e 9, whereas gains are related to chromosome 1 (Figure 10). A great number of structural abnormalities and recurrent rearrangements were also present in all samples. All founded aberrations were grossly unbalanced leading to the formation of several derivative chromosomes in which any specific part could be identified (marker chromosomes). Most markers were present in each of the four samples analyzed. In the F6 sample, additional 3 markers were found. The chromosome arms more frequently involved in the rearrangement were 1p, 1q, 2q, 3q, 6p, 6q, 10q and 11q. The main chromosomal abnormalities observed are listed in Table n°2.

Orthotopic transplantation of 021 GBM-derived neurospheres and clones displayed heterogeneous behavior

To test the tumorigenic potential of 021 GBM-derived neurospheres,

we injected 10^5 of these cells into nude mice. 14 days after implant, we found no signs of tumor bulk but only few infiltrative cells ($n=5$). 25 days after transplantation, few cells are visible near the injection site and accumulation of hemosiderin around the vessels suggesting an increased permeability of the vessels themselves ($n=5$). Only one of this mice showed a progressive neuronal loss and has to be sacrificed. From 45 days ($n=5$) to 65 days ($n=5$) the results are similar to the previous ones: some infiltrative cells, mainly near the injection site. 75 days after implant ($n=6$) we found infiltrating cells along the corpus callosum and in the neighboring parenchyma. Large tumor masses with peripheral infiltration were obtained 100 days after the injection of 021 GBM-derived neurospheres in 6 of 8 injected nude mice (Figure 4A-E). The tumors were characterized by the presence of human lamin A/C positive cells to demonstrate its human origin, co-expressing GFAP (Figure 4G, 4I) and human Ki-67 (Figure 4H), suggesting an active state of proliferation. We also verified whether the tumor progression depend on the number of injected cells. In this sense, we injected 5×10^5 cells obtained from the 021 GBM-derived neurospheres. After 60 days of transplantation, we found several clusters of cells with a nodular aspect, suggesting that cells quantity may influence the time course of the tumors. The incidence of tumors obtained after 100 days from the transplantation of cells isolated from the 021 GBM-derived neurospheres remained however similar (6/8) regardless of the number of cells injected (10^5 and 5×10^5). All these data suggest an intrinsic heterogeneity in tumorigenic properties within the 021 GBM-derived neurospheres that may explain the different tumorigenic effects in xenografts outcomes.

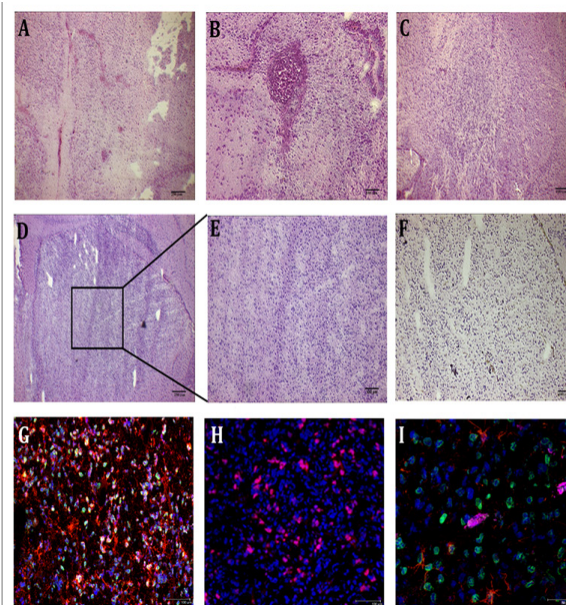


Figure 4 Histopathologic features of tumors generated by the injection of 10^5 cells derived from one GBM biopsy (named 021) in nude mice brain. Slides stained with H&E shows at different time points different degrees of pathologic structures. Parenchymal abnormalities were found 15 days after the injection (A; magnification 4X). 25 days after transplantation, injected brains showed a cluster of proliferating cells with some early infiltration in the neighbouring parenchyma (B; magnification 10X). C, high infiltration of tumoral cells was found 50 days after transplantation (magnification 10X). In D (detailed in E) is evident a large tumor mass with peripheral infiltration, obtained 100 days after the injection (magnification 4X). Few CD31 positive vessels are present in tumor bulk as shown by immunohistochemical analysis (F). Immunofluorescence staining shows the presence of several human lamin A/C positive cells (green) co-expressing GFAP (red) (G,I; magnification 20-40X). Tumor cells were found positive for the human Ki-67 demonstrating a proliferation state *in vivo* (H; magnification 20X).

Table 2 Main chromosomal abnormalities observed*

Line	Mitotic index	Chromosome modal number	Losses	Gains	Deletions	Other structural anomalies	Markers
Biopsy 021 (early passage)	1,58	near tetraploidy 81-103	-2				Mar1
			-7				Mar2
			-9				Mar3
			-10[x2]	1	del(1)(p32) [x3]	der(6)t(2;6)(q11;q26)	Mar4
			-13				mar5 [x2]
			-15				
			-X				
			-5				
Biopsy 021 (P20)		near tetraploidy 81-103	-8				Mar1
			-9 [x2]			der(1)t(1;?)(q10;?)	Mar2
			-10	+1 [x2]	del(1)(p32) [x2]	der(10)t(6;10) (p10;q10)	Mar3
			-11	7	del(1)(q25)	add(11)(q24)	mar4 [x3]
			-15 [x2]				mar5 [x2]
			-17 [x2]				
			-19				
C2 (P3)	0,88	near tetraploidy 81-103	-2				Mar1
			-5 [x2]	+1 [x2]	del(1)(p32)		Mar2
			-9	12	del(1)(q25)	add(11)(q24)	Mar3
			-11	15	del(3)(q21)	der(10)t(6;10) (p10;q10)	Mar4
			-14	18	del(6)(q15)		mar5 [x2]
			-17				
			-1				
			-5				
F6 (P3)	2,37	near tetraploidy 81-103	-6 [x2]				mar2 [x2]
			-8				mar4 [x2]
			-9 [x2]	+12 [x2]	del(1)(p32)	add(3)(q28)	Mar5
			-11 [x2]				Mar6
			-15 [x2]				mar7 [x2]
			-19				Mar8
-20							

*All numerical changes are expressed in relation to the appropriate ploidy level.

To test whether the difference between the proliferation rates of the clones obtained from the 021 GBM-derived neurospheres *in vitro* and in CAM experiment can be recapitulated *in vivo*, we injected 10^5 cell of both the fastest (C2; n=10) and the slowest (F6; n=10) of these clones. Time of analysis was 80 and 100 days. One animal injected with the C2 clone was sacrificed before the end of the experiment due to evident neurological side effects. After 80 days of transplantation of the C2 clone, we found in all injected animals (n=5) a large amount of human lamin A/C positive cells that spread along corpus callosum and infiltrated in the striatum where they create clusters (Figure 5A, 5B). This is especially evident in the animals sacrificed 100 days after transplant (n=5). However, the animals injected with the F6 clone showed very few lamin A/C positive cells, located along corpus callosum or near the injection site. In one of the mice sacrificed after 100 days of transplantation of the F6 clone we did not observe any lamin A/C cell (Figure 5C, 5D). These results suggest the existence of different populations of cancer stem cells within GBM-derived neurospheres that present different growth rate *in vitro* and *in vivo* that could explain the heterogeneous behavior of GBM. In fact, the faster clone *in vitro* gave rise to bigger tumor mass *in vivo* and, *vice versa*, the slower did not form sizeable tumors and sometimes they did not survive in mice brains.

REST and Olig2 expression in 021 GBM-derived clones was heterogeneous

To evaluate the expression of the transcription factors REST and Olig2 of the clones, we performed, as a first step, immunofluorescent staining on cell cytospins (Figure 6A, 6D). The clones showed a high rate of protein expression, the lowest being E7 clone (60%) for REST

and D11 (54%) for Olig2. Interestingly we could observe the opposite REST and Olig2 expression within the single clones, underlying a balance between stemness and commitment toward glial fate (Figure 6B, 6E).

Because almost all the clones showed similar expression and immunofluorescence could not provide solid quantification, we analyzed the levels of the transcription factors by qRT-PCR and focusing on REST and Olig2 mRNA. We reported the results related to the 021 *in toto* mRNA levels, expressed as 100% (Figure 6C, 6F). Differences among the clones were then clearer for both the molecules and we could divide the clones in groups based on the expression levels. Considering REST expression, it was immediately evident the higher value of D11 and C2 clones, which showed a level of mRNA 3 fold increased than 021; the F10 clone was the one expressing the lowest value, the same of *in toto* cells; all the other clones showed values twice higher than the reference 021. As regards Olig2, the clones with the highest expression (3 fold increased) was F6, D11 and E7, followed by C10 (2.5 fold increased) and C2 and F6 (2 fold increased). F10 and C3 were the lowest one, displaying a value slightly similar to 021 mRNA expression. In this analysis, however, the opposite relationship between REST and Olig2 expression was not as evident as for the immunofluorescence results. Western blot analysis of REST confirmed at protein level the results obtained by PCR with significant differences between the faster and the slower of the clones (Figure 6G). These data highlights a straight relationship between proliferation and tumorigenic properties of the clones and REST levels, suggesting a possible role as a prognostic marker of this transcription factor.

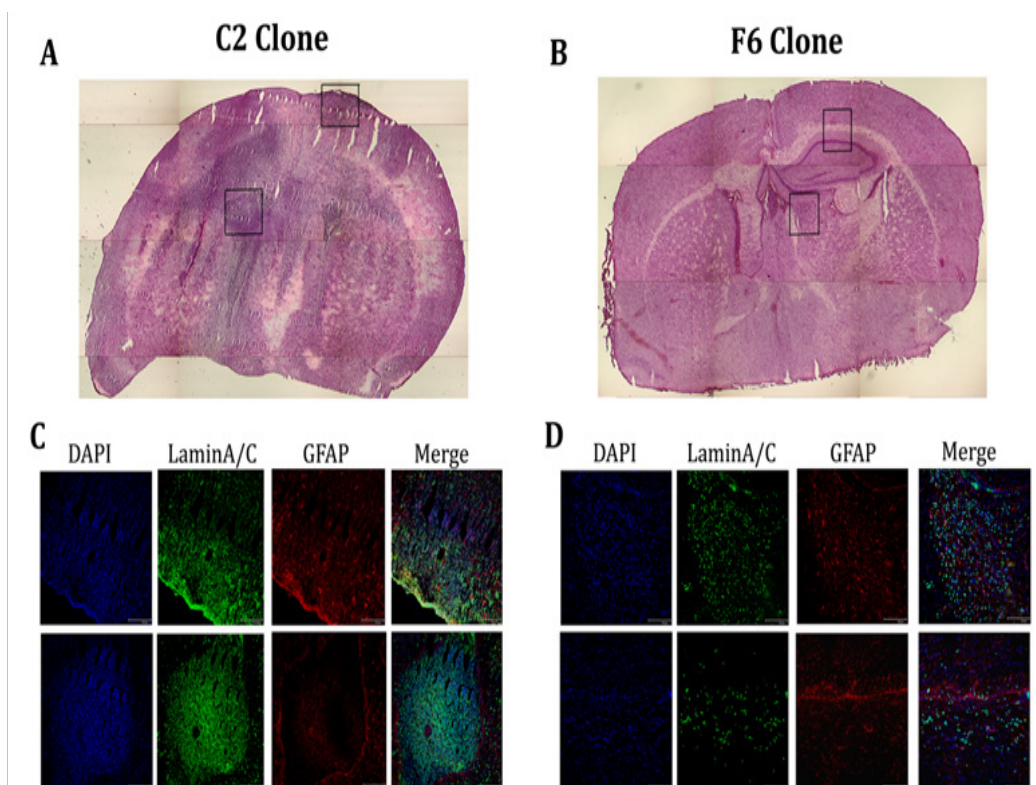


Figure 5 *In vivo* analysis of xenografts experiments performed C2 and F6 clones obtained from the 021 GBM neurospheres. A, B, H&E staining of coronal section of brains injected with C2 clone demonstrates large and infiltrating tumor mass while only few infiltrating cells were present in brains injected with F6 clone (magnification 4X). Quadrants in A and B are detailed in C and D by confocal images representing human lamin A/C positive cells (in green) co-expressing the glial marker GFAP (in red) (magnification 20X).

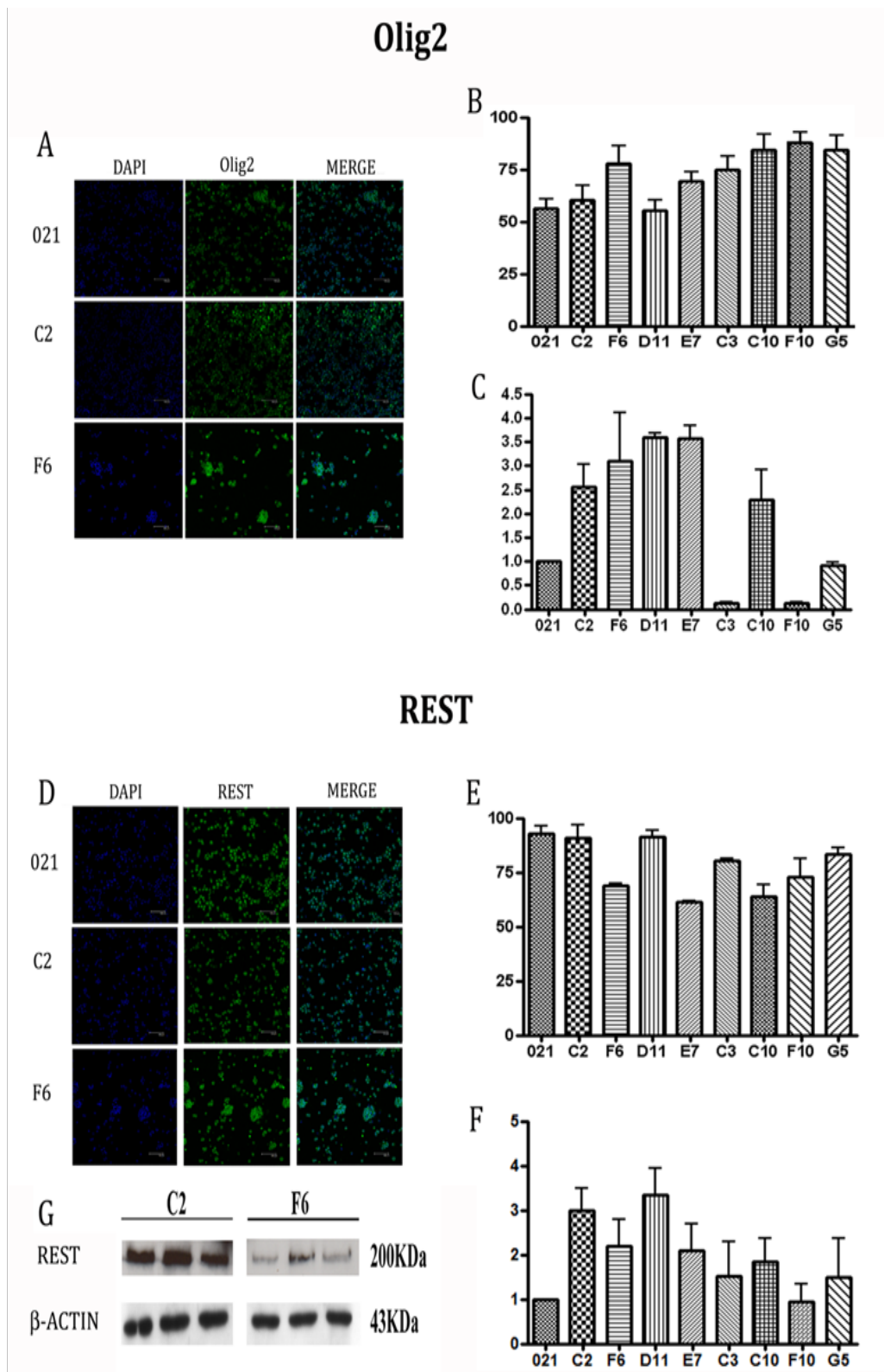


Figure 6 Olig2 and REST expression analyzed with different assays in O21 derived clones. Immunofluorescence staining of Olig2 and REST protein in O21 *in toto*, C2 and F6 derived neurospheres cytopins as representative of all the clones (A,D). Relative percentage of Olig2/REST positive cells that show a general opposite expression of the two factors in the same clone (B,E). Quantification by Real Time PCR of Olig2 and REST mRNA levels; results are related to the O21 *in toto* mRNA levels, expressed as 100% (C,F) and Western blot analysis of C2 and F6 clones (G) reveals the different expression levels that correlates with the proliferative and tumorigenic properties of the clones.

Conclusion

Tumors consist of heterogeneous populations of cells differing in markers expression and growth capacities. The more recent hypothesis suggests that this heterogeneity is because of ongoing differentiation within a tumor. In this model, only a small population of cells is clonogenic and contains tumor initiating potential whereas the majority of the tumor cells have undergone differentiation and lost this potential.^{30,31} These clonogenic tumor cells are capable of inducing a new tumor in mice and are therefore defined as CSCs.³² A possible explanation for this tumor variety is the ability of tumor cells to modify their phenotype during tumor progression, with multiple cohorts of CSCs with different tumor initiating capacity being generated.³³

In our experiments, we firstly isolated neurospheres from different grade brain tumors and verified their stemness properties inducing multilineage differentiation ability and observing in all the samples, independently from the tumor grade, the formation of all the three neural lineage cell type. As we expected and as previously described as aberrant differentiation, under differentiating conditions, CSCs often co-express both neural and astrocytes markers.^{6,7,34} Our *in vivo* experiments, performed with GBM-derived neurospheres showed highly variable outcomes, in term of time of onset and tumor size; we ascribe this result to the relative percentage of more aggressive cells that composed the neurospheres injected. All these observations raise the question as to whether the capacity to generate a heterogeneous tumor resides in a monoclonal cell population or depends on multiple different CSCs. This is especially relevant when considering the multiple differentiation patterns observed in brain tumors, which could be a sign of multilineage differentiation by a CSC, but could also be originated by a polyclonal CSC population in which different cells follow separate differentiation programs. This last hypothesis could correspond to the combination of the cancer stem cell and clonal evolution models. Therefore, we decided to obtain single-cell-cloned CSCs from brain tumor sample (named 021); they maintain all their stemness characteristics showing self-renewal, proliferation and multilineage differentiation as well as aberrant differentiating patterns. Intriguingly, the most interesting evidence emerged during the culture of this clones was the different growth kinetics. This observation firstly highlights the heterogeneity within these cells and suggests different proliferation abilities between clones that may reflect differences in their *in vivo* tumorigenesis. This heterogeneity did not emerge due to *in vitro* culture, as demonstrated by cytogenetic. This analysis showed that these cells maintain a tetraploid-like karyotype, both in the early passages and after several months of *in vitro* culture. Furthermore, the cells maintain the mainly original chromosomal aberration, suggesting the possibility that should behave in different way probably due to the environmental influences or epigenetic mechanisms able to induce behavioral changes in the cells. In this view, and to support confirm the hypothesis about the existence of distinct differentiation staged CSCs population, the evaluation of the REST/NRSF and Olig2 role in regulating the different proliferation kinetics could highlight a possible reason of different regulation in stemness/progenitor fate decision, with REST maintaining the more undifferentiated condition and Olig2 determining the early glial commitment.

We observed a high variability of both protein and mRNA expression of this two regulating factors, as a confirm to the evidenced heterogeneity. In particular, the inverse correlation between the expression of REST and Olig2 within the single clones matches with the diverse differentiation stages of the cells: in the more

differentiated one Olig2 was more expressed than REST, and the more stem-like displayed REST levels higher than Olig2. The balance of the effects of the two transcription factors could determine the proliferation rate because, as known, stem cells divide slower than progenitor or partially committed cells. We could therefore correlate the different proliferation rates with the differentiation stages of the cells; in particular, except for D11 and C10 clones, higher Olig2 values correlate with lower REST levels and vice versa. The clones C3 and F10 mirror exactly our hypothesis; in fact, they expressed higher REST than Olig2 levels and showed an increased proliferation rate. Experiments conducted on CAM and nude mice injections allowed us to confirm the differences observed *in vitro*. In fact, the clones reproduced the same growth speed showed in culture. These evidences supported the idea of the existence of at least two types of tumorigenic cells within the spheres: the fast and the slow tumorigenic cells. Interestingly, we could correlate the tumorigenic properties with the expression of the two transcription factors observing a putative predictive role of REST. As we demonstrated, since REST was up regulated in C2 clone, matched with an increase proliferative potential *in vitro* and more tumorigenic and invasive properties *in vivo*. On the other hand, minor expression of the transcription factor, is linked to a less proliferative and tumorigenic behavior. Olig2, instead, did not show any correlation with tumorigenic properties; it was as we expected, since in a previous work, Ligon and colleagues demonstrated by immunohistochemistry a higher expression in anaplastic oligodendrogliomas versus GBMs, which are heterogeneous with respect to Olig2 levels.²³ These findings confirm the results obtained by Kamal and colleagues about the tumorigenic role of REST, and provide insights about the heterogeneity of glioma tumors, generated by several clones' subtypes. The presence of these different clones with different tumorigenic ability, especially in term of REST expression, could be an important pathway to develop targeted drugs. All these findings evidenced different subpopulations of CSCs originating from the same specimen with different *in vivo* behaviors and reveal that this heterogeneity matches exactly the CSC hypothesis that describes the tumors as hierarchical organization of malignant clones with the clonal evolution that determine uncontrolled proliferation and differentiation of tumor cells.

We demonstrated the existence of cell with diverse differentiation stages within tumor spheres but this findings raise an intriguingly question about the reason why these cells, under apparent identical conditions, would retain stemness in some cells and turn on differentiation programs in others. One of the possible reasons for this question supposes that the regulators driving this heterogeneity are differently active in the different clones, as demonstrated highlighting the different expression levels of REST and Olig2 *in vivo* or *in vitro*. On the basis of these results, underline and deepen the knowledge about the factors driving the differentiation and commitment of CSCs and their mechanisms will be of great interest to better understand the biological and clinical behavior of glial tumors and to develop new more effective therapeutic approaches.

Acknowledgements

We thank the Fondazione IRCCS Ca' Granda Ospedale Maggiore Policlinico (Progetto a Concorso 2008) and the Associazione Amici Centro Dino Ferrari. This work was supported by grant from Italian Ministry of Health (GR-2008-1146615).

Conflicts of interest

No potential conflicts of interests were disclosed.

References

1. Ichim CV, Wells RA. First among equals: the cancer cell hierarchy. *Leuk Lymphoma*. 2006;47(10):2017–2027.
2. Axelson H, Fredlund E, Ovenberger M, et al. Hypoxia-induced dedifferentiation of tumor cells—a mechanism behind heterogeneity and aggressiveness of solid tumors. *Semin Cell Dev Biol*. 2005;16(4–5):554–563.
3. Campbell LL, Polyak K. Breast tumor heterogeneity: cancer stem cells or clonal evolution? *Cell Cycle*. 2007;6(19):2332–2338.
4. Merlo LM, Pepper JW, Reid BJ, et al. Cancer as an evolutionary and ecological process. *Nat Rev Cancer*. 2006;6(5):924–935.
5. Vescovi AL, Galli R, Reynolds BA. Brain tumour stem cells. *Nat Rev Cancer*. 2006;6(6):425–436.
6. Galli R, Binda E, Orfanelli U, et al. Isolation and characterization of tumorigenic, stem-like neural precursors from human glioblastoma. *Cancer Res*. 2004;64(19):7011–7021.
7. Singh SK, Clarke ID, Terasaki M, et al. Identification of a cancer stem cell in human brain tumors. *Cancer Res*. 2003;63(18):5821–5828.
8. Zeppernick F, Ahmadi R, Campos B, et al. Stem cell marker CD133 affects clinical outcome in glioma patients. *Clin Cancer Res*. 2008;14(1):123–129.
9. Phillips HS, Kharbanda S, Chen R, et al. Molecular subclasses of high-grade glioma predict prognosis, delineate a pattern of disease progression, and resemble stages in neurogenesis. *Cancer Cell*. 2006;9(3):157–173.
10. Wang J, Sakariassen PO, Tsinkalovsky O, et al. CD133 negative glioma cells form tumors in nude rats and give rise to CD133 positive cells. *Int J Cancer*. 2008;122(4):761–768.
11. Li L, Neaves WB. Normal stem cells and cancer stem cells: the niche matters. *Cancer Res*. 2006;66(9):4553–4557.
12. Morshead CM, van der Kooy D. Disguising adult neural stem cells. *Curr Opin Neurobiol*. 2004;14(1):125–131.
13. Sanai N, Alvarez-Buylla A, Berger MS. Neural stem cells and the origin of gliomas. *N Engl J Med*. 2005;353(8):811–822.
14. Dean M, Fojo T, Bates S. Tumour stem cells and drug resistance. *Nat Rev Cancer*. 2005;5(4):275–284.
15. Bao S, Wu Q, McLendon RE, et al. Glioma stem cells promote chemoresistance by preferential activation of the DNA damage response. *Nature*. 2006;444(7120):756–760.
16. Johnson R, Teh CH, Kurnarso G, et al. REST regulates distinct transcriptional networks in embryonic and neural stem cells. *PLoS Biol*. 2008;6(10):e256.
17. Schoenherr CJ, Anderson DJ. Silencing is golden: negative regulation in the control of neuronal gene transcription. *Curr Opin Neurobiol*. 1995;5(5):566–571.
18. Singh SK, Kagalwala MN, Parker-Thornburg J, et al. REST maintains self-renewal and pluripotency of embryonic stem cells. *Nature*. 2008;453(7192):223–227.
19. Su X, Gopalakrishnan V, Stearns D, et al. Abnormal expression of REST/NRSF and Myc in neural stem/progenitor cells causes cerebellar tumors by blocking neuronal differentiation. *Mol Cell Biol*. 2006;26(5):1666–1678.
20. Conti L, Crisafulli L, Caldera V, et al. REST controls self-renewal and tumorigenic competence of human glioblastoma cells. *PLoS One*. 2012;7(6):e38486.
21. Kamal MM, Sathyan P, Singh SK, et al. REST regulates oncogenic properties of glioblastoma stem cells. *Stem Cells*. 2012;30(3):405–414.
22. Otero JJ, Rowitch D, Vandenberg S. OLIG2 is differentially expressed in pediatric astrocytic and in ependymal neoplasms. *J Neurooncol*. 2010;104(2):423–438.
23. Ligon KL, Alberta JA, Kho AT, et al. The oligodendroglial lineage marker OLIG2 is universally expressed in diffuse gliomas. *J Neuropathol Exp Neurol*. 2004;63(5):499–509.
24. Gritti A, Parati EA, Cova L, et al. Multipotential stem cells from the adult mouse brain proliferate and self-renew in response to basic fibroblast growth factor. *J Neurosci*. 1996;16(3):1091–1100.
25. Reynolds BA, Weiss S. Generation of neurons and astrocytes from isolated cells of the adult mammalian central nervous system. *Science*. 1992;255(5052):1707–1710.
26. Hagedorn M, Javerzat S, Gilges D, et al. Accessing key steps of human tumor progression in vivo by using an avian embryo model. *Proc Natl Acad Sci U S A*. 2005;102(5):1643–1648.
27. Livak KJ, Schmittgen TD. Analysis of relative gene expression data using real-time quantitative PCR and the 2^{-ΔΔC_T} Method. *Methods*. 2001;25(4):402–408.
28. Lowry OH, Rosebrough NJ, Farr AL, et al. Protein measurement with the Folin phenol reagent. *J Biol Chem*. 1951;193(1):265–275.
29. Pisati F, Belicchi M, Acerbi F, et al. Effect of human skin-derived stem cells on vessel architecture, tumor growth, and tumor invasion in brain tumor animal models. *Cancer Res*. 2007;67(7):3054–3063.
30. Dalerba P, Cho RW, Clarke MF. Cancer stem cells: models and concepts. *Annu Rev Med*. 2007;58:267–284.
31. Vermeulen L, Todaro M, de Sousa Mello F, et al. Single-cell cloning of colon cancer stem cells reveals a multi-lineage differentiation capacity. *Proc Natl Acad Sci U S A*. 2008;105(36):13427–13432.
32. Clarke MF, Dick JE, Dirks PB, et al. Cancer stem cells—perspectives on current status and future directions: AACR Workshop on cancer stem cells. *Cancer Res*. 2006;66(19):9339–9344.
33. Hill RP, Perris R. “Destemming” cancer stem cells. *J Natl Cancer Inst*. 2007;99(19):1435–1440.
34. Ignatova TN, Kukekov VG, Laywell ED, et al. Human cortical glial tumors contain neural stem-like cells expressing astroglial and neuronal markers in vitro. *Glia*. 2002;39(3):193–206.